Electronic Supplementary Material (ESI) for Journal of Materials Chemistry A.

Visible-Light Active Catechol-Metal Oxide Carbonaceous Polymeric Material for Enhanced Photocatalytic Activity

P. Karthik,[1] R. Vinoth,[1] P. Selvam,[2] E. Balaraman,[3]* M. Navaneethan,[4] Y. Hayakawa,[4] and B. Neppolian[1],*

[1]*SRM Research Institute, SRM University, Kattankulathur, Chennai- 603203, Tamil Nadu, India.*
[2]*National Center for Catalysis Research, Department of Chemistry, Indian Institute of Technology - Madras, Chennai - 600036, India.*
[3]*Catalysis Division, CSIR-National Chemical Laboratory (CSIR-NCL), Dr. Homi Bhabha Road, Pune - 411008, India.*
[4]*Research Institute of Electronics, Shizuoka University, 3-5-1 Johoku, Naka-Ku, Hamamatsu, Shizuoka 432-8011, Japan.*

Electronic Supplementary Information (ESI)

Figure S10 Superoxide anion ($O_2^{-\bullet}$) radical determination experiment using Nitroblue tetrazolium (NBT) assay.

Figure S11 Effect of calcinations temperature on the formation of (a) catechol-TiO_2 surface complex and (b) photopolymerized catechol-TiO_2 surface complex.

Figure S12 Effect of calcinations time on the formation of (a) catechol-TiO_2 surface complex and (b) photopolymerized catechol-TiO_2 surface complex.

Table S1: Rate constant values of photocatalytic Cr(VI) reduction.

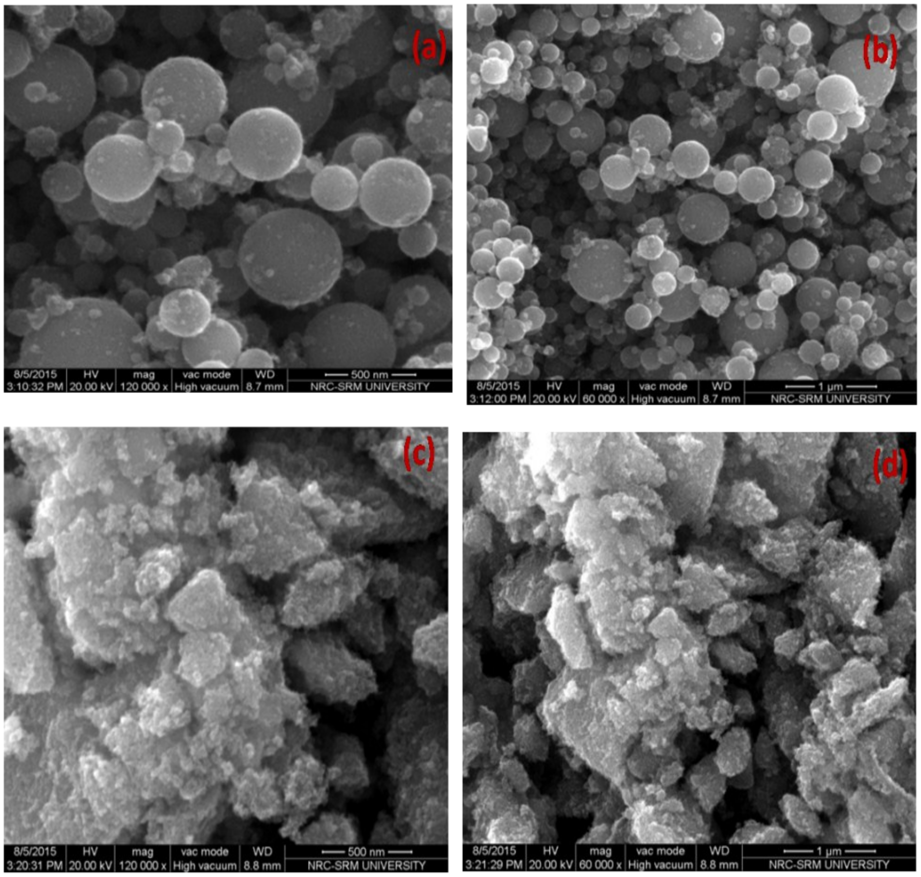

Figure S1 FE-SEM image of (a & b) TiO_2 and (c & d) Catechol-TiO_2 carbonaceous polymer.

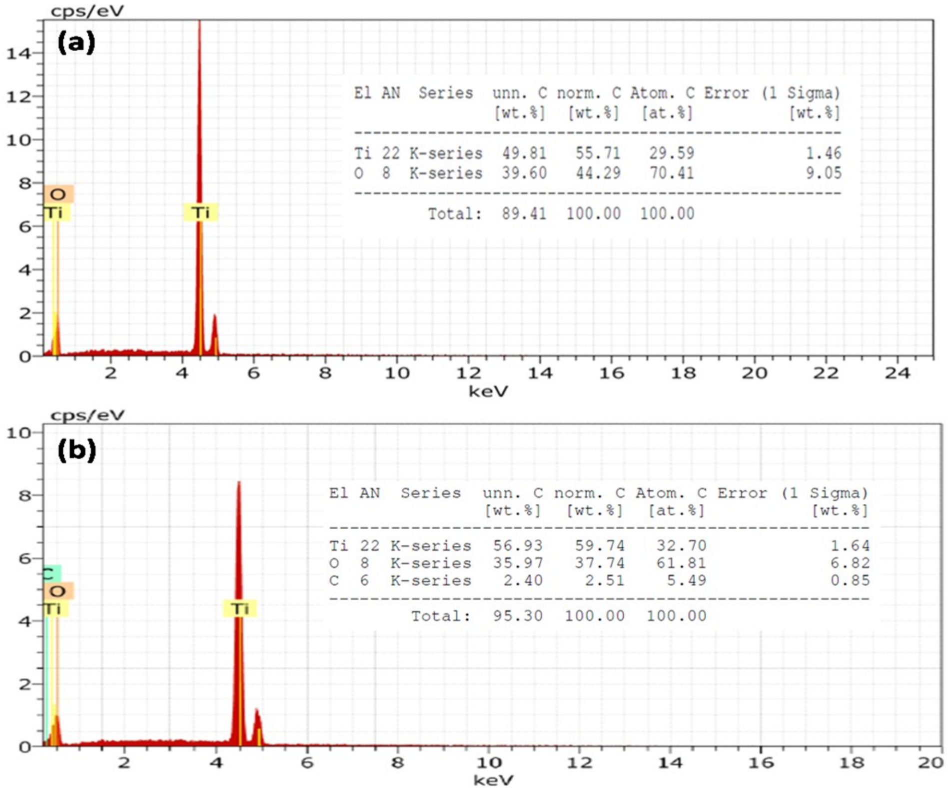

```
El AN  Series   unn. C norm. C Atom. C Error (1 Sigma)
                [wt.%]  [wt.%]  [at.%]           [wt.%]
-----------------------------------------------------
Ti 22 K-series  49.81   55.71   29.59             1.46
O  8  K-series  39.60   44.29   70.41             9.05
-----------------------------------------------------
         Total:  89.41  100.00  100.00
```

```
El AN  Series   unn. C norm. C Atom. C Error (1 Sigma)
                [wt.%]  [wt.%]  [at.%]           [wt.%]
-----------------------------------------------------
Ti 22 K-series  56.93   59.74   32.70             1.64
O  8  K-series  35.97   37.74   61.81             6.82
C  6  K-series   2.40    2.51    5.49             0.85
-----------------------------------------------------
         Total:  95.30  100.00  100.00
```

Figure S2 EDX analysis of (a) TiO_2 (b) Catechol-TiO_2 carbonaceous polymer hybrid.

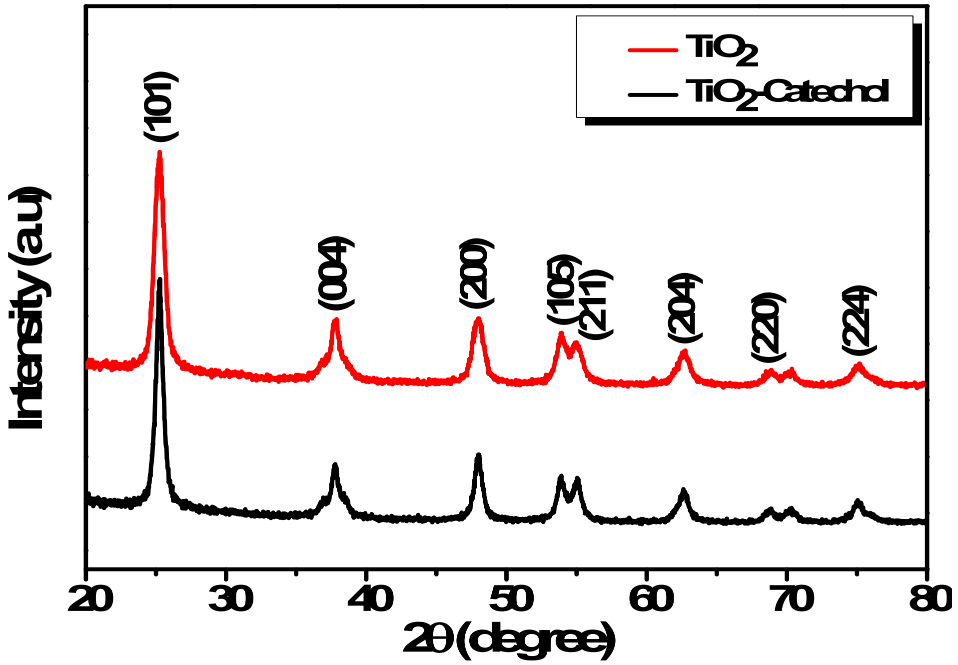

Figure S3 XRD Patterns of TiO_2 and Catechol-TiO_2 carbonaceous polymer.

The phase purity and crystal structure of asprepared TiO_2 and Catechol-TiO_2 carbonaceous polymer were determined by XRD patterns. The XRD patterns of TiO_2 and Catechol functionalized TiO_2 are illustrated in Figure S3. As shown in Figure S3, the characteristic diffraction peaks of ultrasonically prepared mesoporous TiO_2 are 25.1, 37.8, 47.9, 53.9, 55.3, 62.6, 68.8, 70.2, 75.2 and 82.8 correspond to (101), (004), (200), (105), (211), (204), (116), (220), (215) and (224) planes, respectively.[1,2] This clearly indicates the formation of well crystalline anatase phase TiO_2 structure (JCPDS card no.89-4921) and the similar XRD pattern is obtained for TiO_2-Catechol carboneous polymer surface complex. No shift or additional peaks are observed in the existing anatase phase TiO_2. Hence, it confirms that the surface functionalization TiO_2 with catechol linker could not affect or induce new crystalline phase of TiO_2.[3]

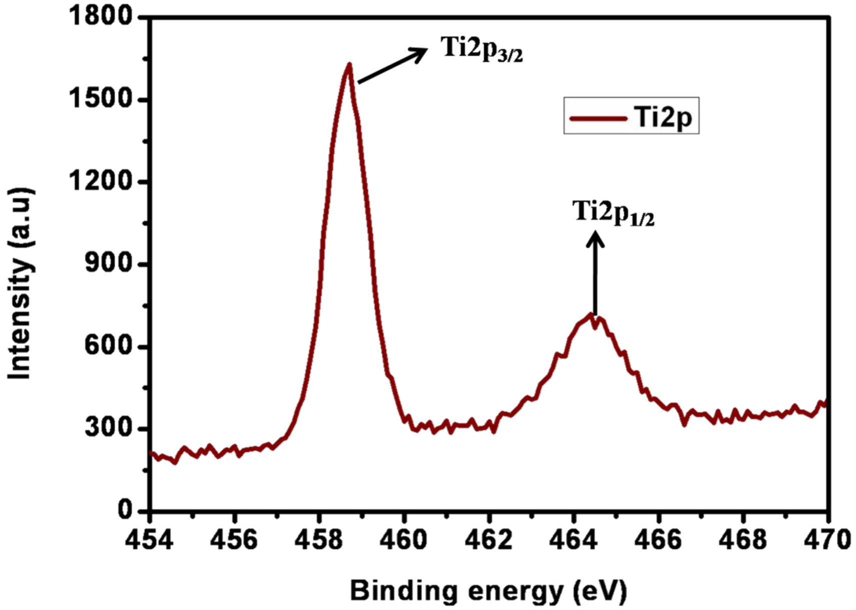

Figure S4 High resolution Ti 2p spectrum of Catechol-TiO_2 carbonaceous polymer.

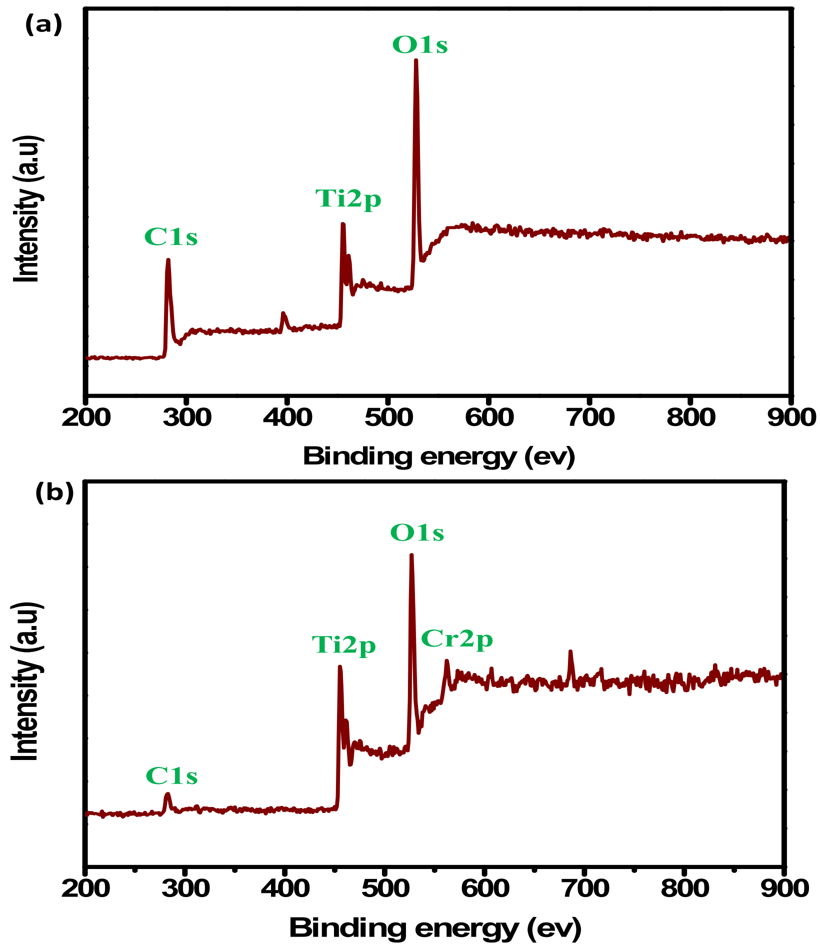

Figure S5 (a) and **(b)** survey scan XPS spectra of before and after photocatalytic reaction.

The survey scan XPS spectra of the Catechol-TiO_2 carbonaceous polymer before and after the photocatalytic Cr (VI) reduction were also performed and are shown in Figure S5. As depicted in Figure S5, the major peaks, such as C1s, O1s, Ti2p and Cr2p are revealed that presence of C, O, Ti and Cr respectively. The binding energy of all the elements was observed in the same region after and before the photocatlytic reaction, further support the high pohotostabilty of photocatalyst. On the other hand, a new peak appeared at 577 eV after the photocatlytic reaction, which can be assigned to Cr (III) ions. The results emphasized that the Cr (VI) ions converted to Cr (III) during photocataytic reduction and reduced Cr (III) ions are adsorbed on the catalyst surface.[4]

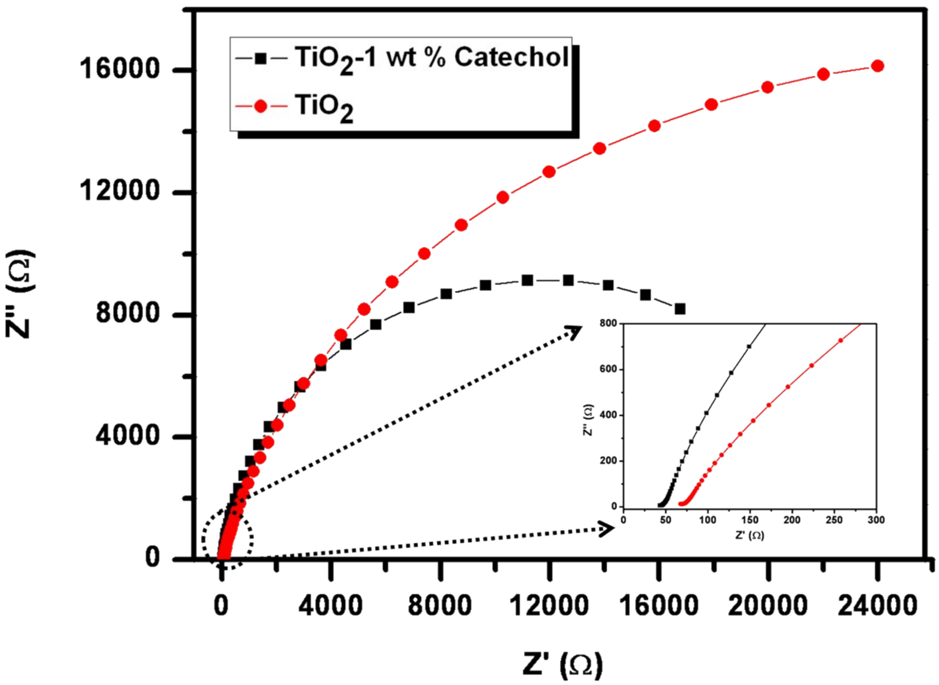

Figure S6 Nyquist plots of TiO2 and 1 wt % Catechol-TiO_2 carbonaceous polymer.

The interfacial charge transport and separation of TiO_2 and Catechol-TiO_2 carbonaceous polymer was investigated through electrochemical impedance analysis (ESI). In general, smaller the arc radius can increase carrier separation at the interface[2]. As shown in Figure S5, the arc radius of Catechol-TiO_2 carbonaceous polymer is comparatively smaller than TiO_2, which indicates that introduction of catechol increase the charge separation efficiency at interface and thereby enhance photocatalytic activity.

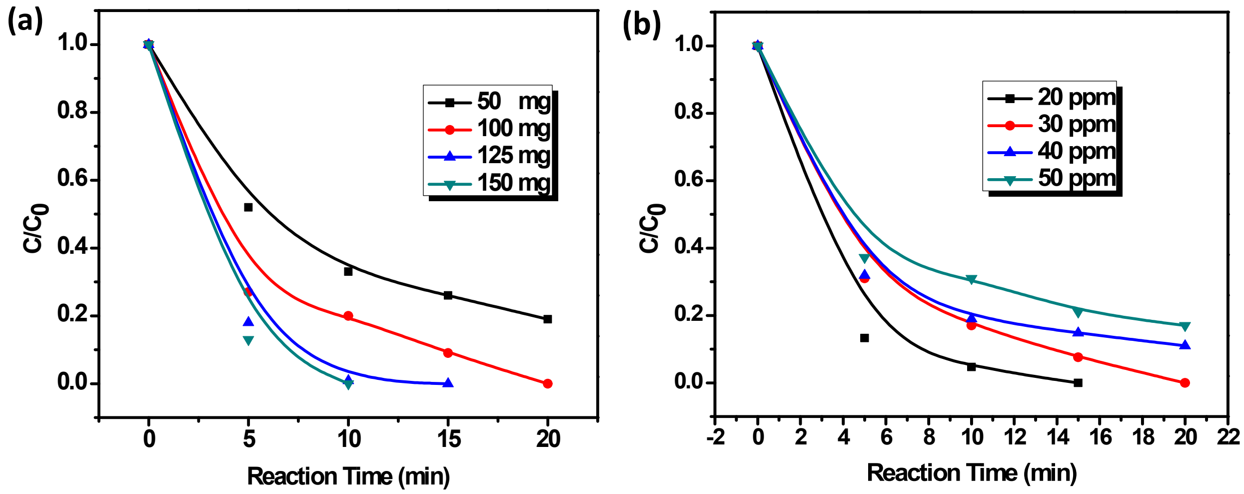

Figure S7 (a) different catalyst loading **(b)** Effect of different initial concentration of Cr (VI).

To study the effect of initial concentration of Cr (VI) on photoctatalysis, the photocatalytic reaction was carried out with different initial concentrations (20, 30, 40, 50 ppm) of Cr (VI). The rate of the reaction change with respect to the initial concentration of Cr (VI) and irradiation time is shown in Figure S7. The rate of photocatalytic reduction is decreasing from 100 to 66 % by increasing the initial concentration of Cr (VI) from 20-50 ppm. The rate constant for the photoreduction reaction with different initial concentration of Cr (VI) were calculated from Figure S7, and the values are given in Table 1. As given from the table 1, the rate constant values are decreasing with increasing the initial concentration of Cr (VI). It is clearly indicated that the rate of the reaction is significantly affected by concentration of Cr (VI) and it follows the pseudo first order kinetics. Since, the main reason for decreasing the photocatalytic activity is that the photo reduced Cr (III) ions can inhabit on the catalytic active sites and it may decrease the rate of reaction.[5,6] Moreover, the other possible explanation is that the increase in the initial concentration of Cr (VI) can prevent the penetration of light to the surface of photocatalysts.[7]

To examine the effect of different loading of photocatalyst on the rate of photocatalytic reduction reaction, the photocatalytic reaction was carried out with different amount of catalyst loading (50 to 150 mg) under similar experimental conditions. As can be seen from Figure S6, the photocatalytic chromium(VI) reduction rate is increasing with increasing the catalyst loading. However, loading of 125 and 150 mg of photocatalyst, 100% reduction of Cr (VI) was observed within 10 and 15 mins. Since, the increasing the rate of reaction can be justified that the higher amount of photocatalyst loading can absorbs more incident light and it will stimulate the ligand to metal charge transition (LMCT) between catechol to TiO_2, which facilitate high photocatalytic reduction activity.

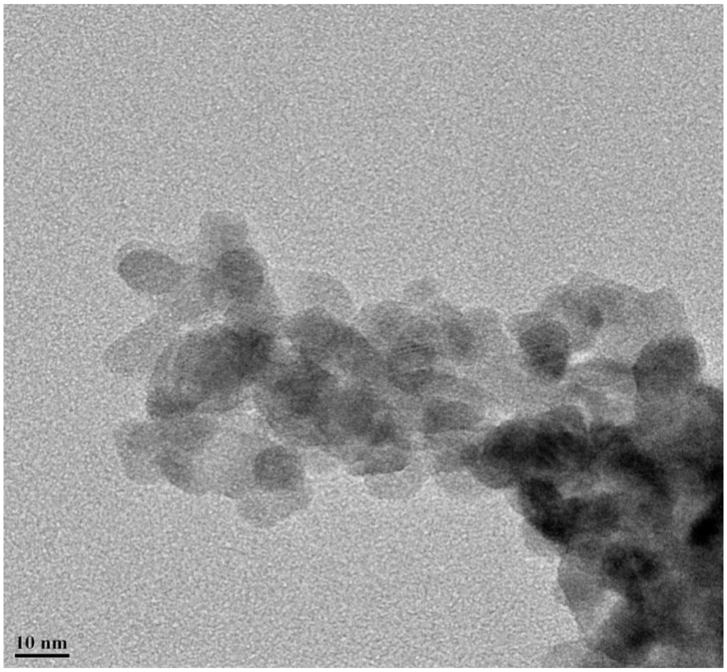

Figure S8 TEM image of Catechol-TiO_2 carbonaceous polymer after five cycles of Cr(VI) reduction.

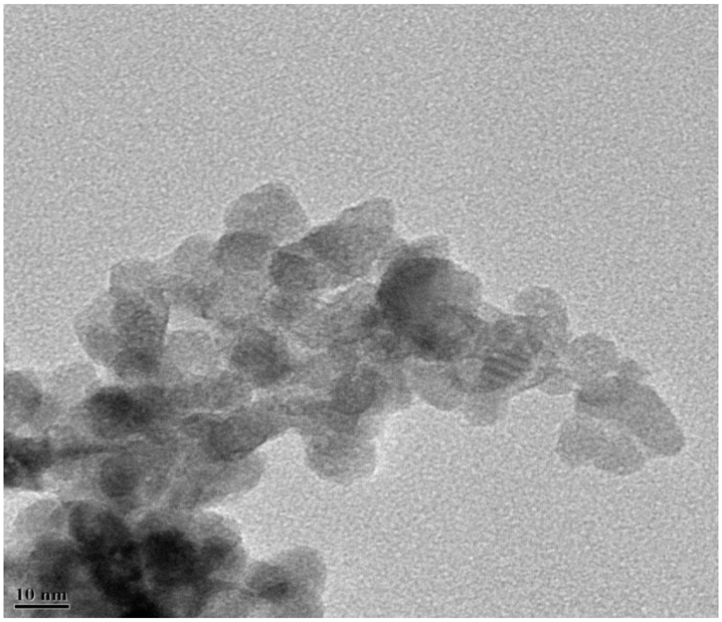

Figure S9 TEM image of Catechol-TiO_2 carbonaceous polymer after three cycles of H_2 production.

Determination of superoxide anion ($O_2^{-\bullet}$) formation experiment

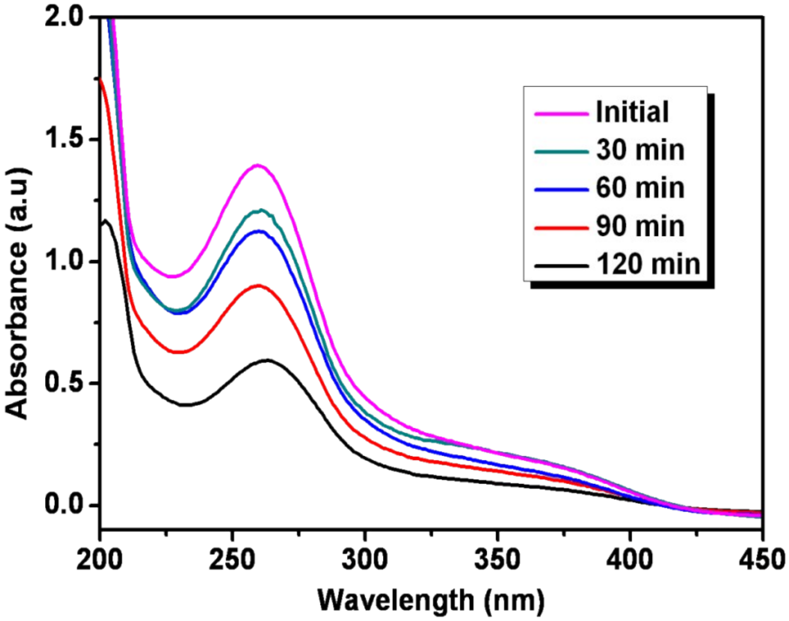

Figure S10 Superoxide anion ($O_2^{-\bullet}$) radical determination experiment using Nitroblue tetrazolium (NBT) assay.

The superoxide anion ($O_2^{-•}$) formation during visible light illumination was confirmed using Nitroblue tetrazolium (NBT) as a selective $O_2^{-•}$ radicals scavenger. The photopolymerization reaction was performed in 25 ppm aqueous NBT solution in the presence of visible light irradiation. The NBT can effectively scavenge the photogenerated $O_2^{-•}$ radicals and it forms insoluble purple formazan as precipitate.[8] The $O_2^{-•}$ radicals formation was analyzed through decreasing the absorbance of NBT at 259 nm. As depicted in Fig. S10, the absorbance of NBT at 259 nm is considerably decreased with increasing irradiation time. This observation clearly reveals that the photogenerated $O_2^{-•}$ radicals react with NBT and thereby decreases the absorbance of NBT. Hence, it supports the effective formation of $O_2^{-•}$ radicals during photopolymerization reaction.

Effect of calcination temperature:

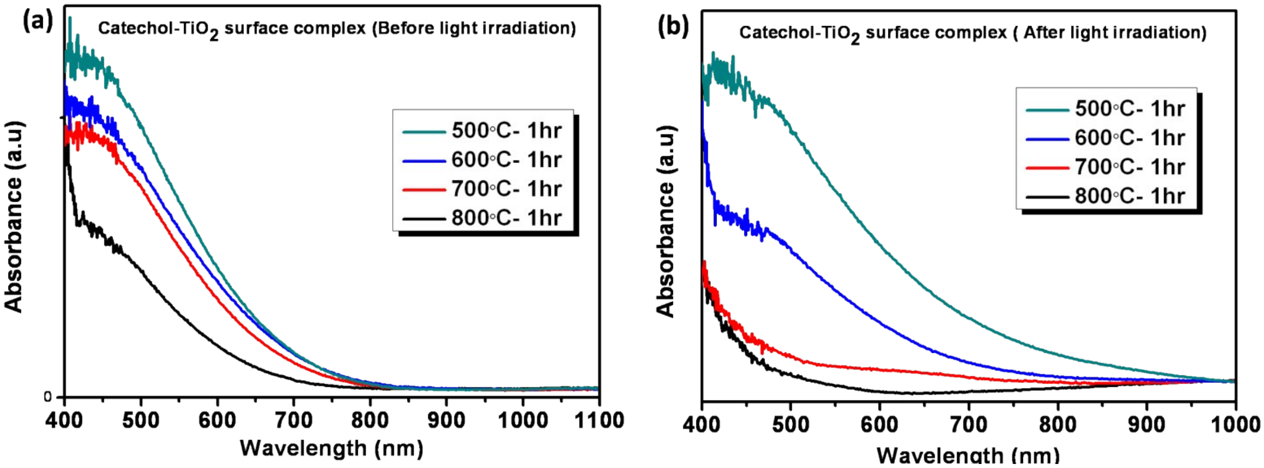

Figure S11 Effect of calcinations temperature on the formation of (a) catechol-TiO_2 surface complex and (b) photopolymerized catechol-TiO_2 surface complex.

The effect of calcination temperature on the formation of surface complex and photopolymerization reaction were demonstrated through various control experiments. Initially, a set of TiO_2 nanoparticles were synthesized with different calcinations temperature varying from 500 to 800 °C. Then, the surface complex formation and photopolymerization reaction were performed with pre-calcinated TiO_2 nanoparticles under identical experimental conditions already described in the experimental section part of the main manuscript. Fig. S11 (a) shows the UV-Vis absorption spectra of catechol-TiO_2 surface complex. The absorbance of TiO_2-surface complex decreases with respect to the increasing calcination temperature. This result clearly confirmed that the surface hydroxyl groups present on TiO_2 play a vital role on the formation of TiO_2-catechol surface complex. On the other hand, the decrease in the absorbance indicates that the calcination temperature considerably reduces the hydroxyl groups and thereby greatly affects the surface complex formation between hydroxyl groups of TiO_2 and catechol[9-12] Similarly, photopolymerization reaction was carried out on the same catechol-TiO_2 surface complexes prepared with different temperature calcinated TiO_2. It is clearly seen from Fig. S 11(b) that the photopolymerized catechol-TiO_2 surface complex not only exhibits enhanced optical absorption but also shows red shift in the absorption edge compare to that of pure catechol-TiO_2 (*before photopolymerization*) surface complexes and further confirms the photopolymerization process. Hence, it was found that low calcination temperature (400 ºC) favor for the effective surface complexation formation due to the high hydroxyl group density.

Effect of calcination time:

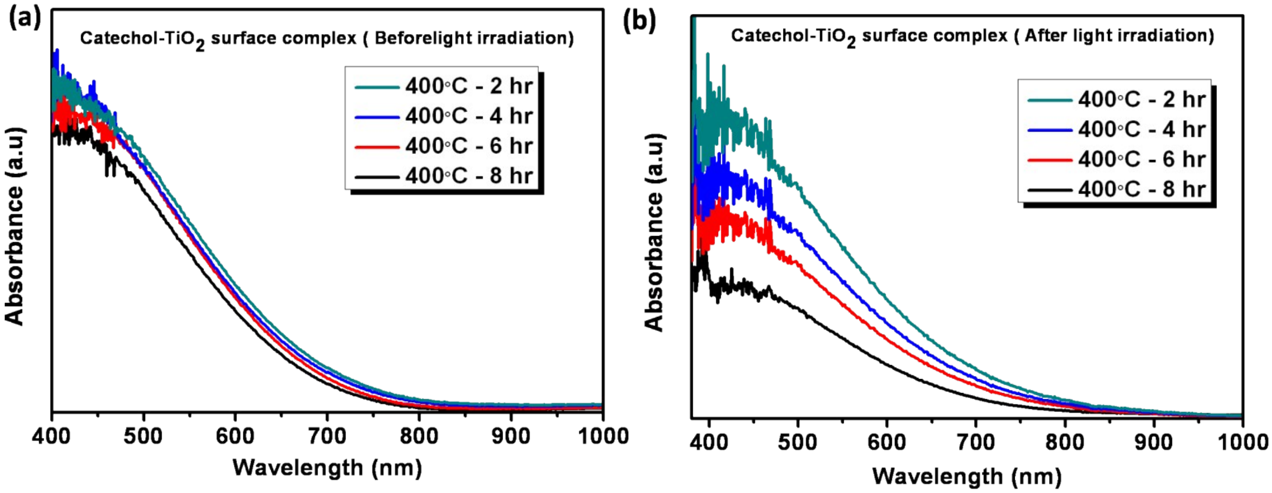

Figure S12 Effect of calcinations time on the formation of (a) catechol-TiO_2 surface complex and (b) photopolymerized catechol-TiO_2 surface complex.

Similarly, the effect of calcination time (2, 4, 6 and 8 h) on the formation of surface complex and photopolymerization reaction were also studied. As shown in Fig. S12 (a&b), the decrease in the optical absorption with respect to increasing calcination time indicates the reduction of surface hydroxyl groups of TiO_2. After the photopolymerization reaction, the decreased absorption with increase of calcination time suggests the effect of calcination time on the formation of photopolymerized catechol-TiO_2 surface complex.

Table. S1 Rate constant values of photocatalytic Cr(VI) reduction

S. No	Initial concentration of Cr(VI) in ppm	K (min^{-1})
1	20	0.3070
2	30	0.1654
3	40	0.1002
4	50	0.0812

Apparent Quantum Yield (AQY):

The AQY was calculated under identical experimental conditions using 420 nm band-pass filters. The light intensity was measured using a lux meter. The irradiation area was calculated as 0.00144 m^2. The calculated AQY values of TiO_2, different wt% catechol polymerized TiO_2 photocatalysts are displayed in Table S2. The optimized 1.0 wt % catechol-TiO_2 carbonaceous polymer photocatalyst shows a highest AQY (59.3 %) compared to that of other photocatalysts. Thus, it clearly demonstrates that the 1.0 wt % catechol-TiO_2 carbonaceous polymer photocatalyst effectively utilize the photons and thereby enhanced the photocatalytic H_2 production rate.

Table S2. Apparent quantum yield (AQY) of TiO_2 and different wt% catechol polymerized TiO_2 photocatalysts.

S. No	Photocatalyst	AQY (%)
1	TiO_2	7.2
2	0.5 wt % Catechol-TiO_2 carbonaceous polymer	26.1
3	0.75 wt % Catechol-TiO_2 carbonaceous polymer	44.6
4	1.0 wt % Catechol-TiO_2 carbonaceous polymer	59.3
5	2.0 wt % Catechol-TiO_2 carbonaceous polymer	31.5
6	3.0 wt % Catechol-TiO_2 carbonaceous polymer	39.2

AQY calculation details

The energy of one photon (E_{photon}) with wavelength of λ_{inc} (nm) is calculated using the following equation.[13]

$$E_{photon} = \frac{hc}{\lambda_{inc}}$$

Where,

h - Planck's constant (J·s)

c - Speed of light (m s^{-1})

λ_{inc} - wavelength of the incident monochromatic light (m)

Total energy of the incident monochromatic light (E_{total})[13]is calculated using the following equation,

$$E_{total} = PSt$$

Where,

P - Power density of the incident monochromatic light (W/m^2)

S - Irradiation area (m^2)

t- Duration of the incident light exposure (s)

The number of incident photons can be obtained through the following equation,

$$\text{Number of incident photons} = \frac{E_{total}}{E_{photon}} = \frac{PS\,\lambda_{inc}t}{hc}$$

Quantum yield (Q.Y.) which is widely used to evaluate the performance of photocatalysts for water splitting, is defined by the following equation

$$\text{Q.Y.(\%)} = \frac{Q.Y.(\%)\ Number\ of\ reacted\ electrons}{Number\ of\ incident\ photons} \times 100$$

However, it is difficult to directly determine the number of reacted electrons *via* experimental methods. As a result, the apparent quantum yield (A.Q.Y.) is defined as follow by substituting twice the number of H_2 molecules evolved for the number of reacted electrons

$$\text{A.Q.Y.(\%)} = \frac{2\ (Number\ of\ H_2\ molecules\ evolved)}{Number\ of\ incident\ photons} \times 100$$

The light intensity was measured using lux meter and converted into power with following equation.[14]

P (W) = (Ev × A) / η

Where,

Ev- Illuminance (lux)

A - Area (m^2)

H- Luminous efficacy (lm/W) for 420 nm (2.732)

References:

1. B. Neppolian, Q. Wang, H. Jung and H. Choi, *Ultrason. Sonochem.*, 2008, **15**, 649.

2. R. Vinoth, P. Karthik, C. Muthamizhchelvan, B. Neppolian, M. Ashokkumar, *Phys. Chem. Chem. Phys.,* 2016,**18**, 5179.

3. A. Akyol, H. C. Yatmaz and M. Bayramoglu, *Appl. Catal., B,* 2004, **54**, 19.

4. L. Shao, J. Li, X. Liang, T. Xie, S. Meng, D. Jiang and M. Chen, *RSC Adv*., 2016, **6**, 1822.

5. A. Akyol, H. C. Yatmaz and M. Bayramoglu, *Appl. Catal., B*, 2004, **54**, 19.

6. M. S. Siboni, M. Farrokhi, R. D. C. Soltani, A. Khataee and S. Tajassosi*, Ind. Eng. Chem. Res*., 2014, **53**, 1079.

7. M. Qamara, M. A. Gondala and Z. H. Yamania, *J. Mol. Catal. A: Chem*., 2011, **341**, 83.

8. A. Czoska, S. Livraghi, M. Chiesa, E. Giamello, S. Agnoli, G. Granozzi, E. Finazzi, C. D. Valentin and G. Pacchioni, *J. Phys. Chem. C,* 2008, **112**, 8951.

9. H. Kim and W. Choi, *Appl. Catal., B,* 2007, **69**, 127.

10. L. Ye, K. Deng, F. Xu, L. Tian, T. Peng and L. Zan, *Phys. Chem. Chem,* 2012, **14**, 82.

11. J. Yu, C. Y. Jimmy, W. Ho and Z. Jiang, *New J. Chem,* 2002, **26**, 607.

12. J.-G. Yu, H.-G. Yu, B. Cheng, X.-J. Zhao, J. C. Yu and W.-K. Ho, *J. Phys. Chem. B,* 2003, **107**, 13871.

13. Y.-G. Yu, G. Chen, L.-X. Hao, Y.-S. Zhou, Y. Wang, J. Pei, J.-X. Sun, Z.-H. Han, *Chem.Commun*., 2013, **49**, 10142.

14. W. R. Siah, H. O. Lintang, M. Shamsuddin, H. Yoshida, L. Yuliati, *Catal. Sci. Tech*., 2016, **6**, 5079.